J. Plasma Physics (1998), *vol.* 59, *part* 3, *pp.* 561–574. Printed in the United Kingdom
© 1998 Cambridge University Press

Linear and nonlinear dust-acoustic waves in non-ideal dusty plasmas

N. N. RAO†

Theoretical Physics Division, Physical Research Laboratory, Navrangpura, Ahmedabad 380009, India

(Received 28 August 1997 and in revised form 20 October 1997)

Linear and nonlinear dust-acoustic wave propagation in a non-ideal classical dusty plasma consisting of electrons, ions and dust grains is investigated by incorporating the van der Waals equation of state for the dust component. For linear waves, it is found from the normal mode dispersion relation that the volume reduction coefficient enhances the phase speed of the dust-acoustic waves, while the molecular cohesive forces lead to a decrease in the phase speed. The relative magnitudes of the two contributions depend on the specific parameter regimes characterizing the non-ideal nature of the dust component. In the high-temperature limit, there is a net increase in the dust-acoustic phase speed, while near the critical point the phase speed is reduced when compared with that for the ideal-gas case. For large amplitudes, we discuss the existence of dust-acoustic solitons by deriving the exact Sagdeev potential. While supersonic solitons are found to be admissible in both the sub- and supercritical parameter regimes, subsonic propagation near the dust-acoustic speed is possible only for the supercritical case. For small but finite amplitudes, explicit analytical solutions have been obtained. A limiting case of these solutions is also discussed.

1. Introduction

Dust is a ubiquitous component of matter encountered in laboratory as well as in terrestrial and astrophysical situations. Quite often, the dust component is embedded in ionized matter, in which case the particles are typically highly charged owing to processes such as electron attachment, plasma current flow and field emission. Charged dust components appear naturally in space environments such as planetary rings, cometary surroundings, interstellar clouds and the lower parts of the Earth's ionosphere (Goertz 1989; Havnes *et al.* 1992). In the laboratory, the dust particles appear as impurities and can significantly influence the behaviour of the surrounding plasma. For example, in tokamak edge plasmas, dust particles can give rise to instabilities resulting in enhanced anomalous diffusion, which is detrimental to plasma confinement (Benkadda *et al.* 1995). Trapped dust impurities lead to serious contamination problems during plasma-aided manufacture of semiconductors (Carlile *et al.* 1991; Bouchoule *et al.* 1991; Sheehan *et al.* 1990). The study of dusty plasmas has developed rapidly over the last few years, with diverse applications in

† E-mail: raonn@prl.ernet.in.

https://doi.org/10.1017/S0022377898006473 Published online by Cambridge University Press

laboratory as well as space plasmas. The field has been reviewed by Mendis and Rosenberg (1994) and Verheest (1996).

Dusty plasmas are multicomponent plasmas that consist, in addition to electrons and ions, of charged finite-sized grains typically in the micrometre range. However, there are three important features that distinguish dusty plasmas from the usual multicomponent plasmas, which have either more than one kind of ion species or electron species with different temperatures.

First, the dust grains are many orders of magnitude heavier than the usual ions, and therefore their mass-to-charge ratio is very large compared with that of the ions or electrons. Hence the plasma frequencies as well as the gyrofrequencies of the ions and the dust particles are widely separated, and consequently it is possible to distinguish the normal modes arising owing to the dust and the ion inertial effects. In fact, in the very low-frequency regime, dusty plasmas support new kinds of normal modes, such as dust-acoustic waves (DAWs) (Rao *et al.* 1990), wherein the inertia as well as the wave dynamics is provided by the dust component. Experiments in dusty laboratory plasmas (Chu *et al.* 1994; D'Angelo 1995; Barkan *et al.* 1995; Pieper and Goree 1996; Prabhuram and Goree 1996; Prabhakara and Tanna 1996) have established the existence of DAWs. In recent years, a number of authors have theoretically investigated various collective processes such as waves and instabilities in dusty plasmas (de Angelis *et al.* 1988; Shukla and Silin 1992; D'Angelo 1993; Bharuthram and Shukla 1992*a*,*b*; Shukla 1992; Rosenberg 1993; Rao 1993*a*,*b*; Rawat and Rao 1993; Motschmann *et al.* 1994; Verheest 1996).

Secondly, the charge on the dust particles can vary either because of wave-motion-induced electron and ion currents flowing onto the grain surface or because of equilibrium charging processes. Thus the dust-grain charge becomes a new dynamical variable, leading to certain new effects in dusty plasmas that are absent in the usual kind of multicomponent plasmas. For example, it has been shown that grain charge fluctuations typically give rise to damping of the waves, which would otherwise propagate as normal modes (Varma *et al.* 1993; Melandsø *et al.* 1993; Rao and Shukla 1994; Jana *et al.* 1994).

The third distinguishing feature is directly related to the large size of the grains, which makes dusty plasmas non-ideal (Fortov and Iakubov 1990). Most analyses have assumed dusty plasmas to be ideal, and thus have neglected effects due to the finite grain size. Such an approximation is valid for grains in the submicrometre range and for dilute plasmas when the characteristic potential energy due to the Coulomb interaction is small compared with the mean thermal energy. However, for larger grain sizes in the supermicrometre range, and particularly at higher gas densities, the mean distance between the particles decreases and hence the interaction between neighbouring particles is enhanced. Thus dusty plasmas consisting of large-sized particulate matter are essentially strongly coupled, and the contributions due to the non-ideal nature of the dusty plasmas may not be negligible. For example, for grains with a radius of about 50 μm, the volume reduction factor is about 10% when the gas density is about 10^5 particles cm^{-3}. Such parameter regimes are within the scope of present-day laboratory experiments on dusty plasmas.

There are several physical mechanisms that can give rise to cohesive forces between the dust particles (Melandsø and Goree 1995; Nambu *et al.* 1995; Shukla and Rao 1996). For example, charge polarization by creation of image charges occurs when particles of finite size approach each other. This can result in attractive forces

https://doi.org/10.1017/S0022377898006473 Published online by Cambridge University Press

between the dust grains, whose magnitudes depend on the intergrain distance as well as the net charges on the grain surfaces. In a high-density non-ideal plasma, this effect may be appreciable. Recent simulations of the interaction of finite-sized charged bodies with a flowing plasma (Melandsø and Goree 1995) indicate the existence of asymmetric screening potentials around the objects. On the other hand, charged particles with the same polarity can attract each other owing to collective interactions involving very low-frequency density fluctuations (Nambu *et al.* 1995; Shukla and Rao 1996) arising from the normal modes such as the DAWs. This effect can be substantial for strongly coupled plasmas, where dust-crystal formation has been observed experimentally.

Dusty plasmas are known to exhibit new properties in the strong-coupling regime. For example, laboratory experiments (Chu and Lin 1994; Thomas *et al.* 1994; Hayashi and Tachibana 1994) have established the formation of plasma crystals in strongly coupled dusty plasmas as a result of Coulomb crystallization, which was first theoretically predicted by Ikezi (1986). Wave-propagation phenomena in strongly coupled non-ideal dusty plasmas is a topic that has not yet been studied extensively in the literature.

In this paper, we present an investigation into the propagation of linear as well as nonlinear DAWs in a nonideal dusty plasma in the classical regime. We assume the electrons and the ions to behave like ideal fluids, whereas the dust component can be described by a suitable equation of state. While there exist different types of non-ideal equations of state, we consider, in order to keep the analysis tractable, the van der Waals equation of state, which is one of the simplest and the most studied in gas kinetic theory. Our results show that the contributions due to the non-ideal equation of state are of two types. For linear normal modes, the volume reduction factor typically leads to an increase in the phase speed of the waves, while the effect of the cohesive forces is to reduce the phase speed. The relative magnitudes of the two contributions depend on the specific parameters of the dust component, and accordingly there could be a net decrease or increase in the DAW phase speed, depending on the parameter regime. On the other hand, for large amplitudes, the parameter regime for the existence of nonlinears DAW is significantly modified.

The paper is organized in the following manner. In Sec. 2 we present the basic equations that govern DAW propagation. In Sec. 3, we derive the normal-mode dispersion relation for the DAW and discuss the contributions due to the non-ideal dust component. In Sec. 4, the existence of nonlinear DAWs is considered. For large amplitudes, the basic equations are reduced to quadrature, while for small but finite amplitudes analytical solutions for DAW solitons are obtained. The main results of the present investigation are summarized in Sec. 5.

2. Basic equations

We consider one-dimensional propagation (along the $\hat{\mathbf{x}}$ direction) of DAWs in a dusty plasma consisting of electrons, ions and finite-sized dust grains. For low-frequencies such that the wave phase speed ω/k is much smaller than the electron and ion thermal speeds (v_{te} and v_{ti} respectively), we use the dusty-plasma model suggested by Rao *et al.* (1990), wherein the electrons and ions are assumed to behave like ideal fluids and to be in thermal equilibrium at their respective temperatures T_e and T_i in the presence of the self-consistent electrostatic field ϕ. Thus the electron

https://doi.org/10.1017/S0022377898006473 Published online by Cambridge University Press

and ion number densities are given respectively by the Boltzmann distributions

$$n_e = n_{e0} \exp\left(\frac{e\phi}{k_B T_e}\right), \quad n_i = n_{i0} \exp\left(-\frac{e\phi}{k_B T_i}\right), \tag{1}$$

where n_{e0} and n_{i0} are the respective equilibrium values, e is the magnitude of the electron charge and k_B is the Boltzmann constant.

For DAWs, the inertia is provided by the heavier dust component, and hence the wave dynamics is governed by the full set of dust fluid equations coupled to the Poisson equation. Accordingly, the relevant basic equations are

$$\frac{\partial n_d}{\partial t} + \frac{\partial}{\partial x}(n_d v_d) = 0, \tag{2}$$

$$m_d n_d \left(\frac{\partial v_d}{\partial t} + v_d \frac{\partial v_d}{\partial x}\right) = -Z_d n_d e \frac{\partial \phi}{\partial x} - \frac{\partial p_d}{\partial x}, \tag{3}$$

$$\frac{\partial^2 \phi}{\partial x^2} = -4\pi e(Z_d n_d + n_i - n_e), \tag{4}$$

where the notation is standard, the subscript d refers to the dust component, and Z_d is the charge number, which is positive (negative) for positively (negatively) charged dust grains.

The system (1)–(4) must be closed by employing a suitable equation of state for the dust component. While the present analysis can be carried out for general equations of state discussed in the literature, we use below, to keep the analysis simple, the well-known van der Waals equation of state, namely

$$\left(p_d + \frac{a}{v_m^2}\right)(v_m - b) = R_d T_d, \tag{5}$$

where v_m is the molar volume, and a, b and R_d are the usual gas constants (Kennard 1938; Hirschfelder *et al.* 1954; Kahn 1965). In terms of the dust number density $n_d \equiv L/v_m$, where L is the Avagadro number, (5) can be rewritten as

$$(p_d + A n_d^2)(1 - B\, n_d) = n_d\, k_d T_d, \tag{6}$$

where $A = a/L^2$, $B = b/L$ and $k_d = R_d/L$. Note that for an ideal dust gas, $k_d \equiv k_B$, and (6) reduces to the usual ideal-gas law when $A = B = 0$. The constants A and B can be calculated in terms of the critical parameters (Joos 1986) by requiring that $\partial p_d/\partial n_d = 0$ and $\partial^2 p_d/\partial n_d^2 = 0$. This yields the relations

$$A = \frac{9}{8}\frac{k_d T_c}{n_c}, \qquad B = \frac{1}{3\, n_c}, \tag{7}$$

where the subscript c denotes the respective values at the critical point.

Equations (1)–(4) and (6) constitute the complete set of basic equations of the present model for non-ideal dusty plasmas. In the next section, we discuss the propagation of linear DAWs.

3. Linear waves

For a linear DAW, the basic equations (1)–(4) and (6) can be analysed by using the standard normal-mode analysis, which yields the dispersion relation

$$\frac{\omega^2}{k^2} = \frac{\omega_{pd}^2 \lambda_D^2}{1 + k^2 \lambda_D^2} + V_{td}^2 + \frac{1}{m_d}\left[B n_{d0} k_d T_d \frac{2 - B n_{d0}}{(1 - B n_{d0})^2} - 2A n_{d0}\right], \tag{8}$$

https://doi.org/10.1017/S0022377898006473 Published online by Cambridge University Press

where $\omega_{pd} = (4\pi n_{d0} Z_d^2 e^2/m_d)^{1/2}$ is the dust plasma frequency, n_{d0} is the equilibrium dust number density and $V_{td} = (k_d T_d/m_d)^{1/2}$ is the dust thermal speed, and the effective Debye length λ_D is defined by

$$\frac{1}{\lambda_D^2} \equiv \frac{1}{\lambda_{De}^2} + \frac{1}{\lambda_{Di}^2} = \frac{4\pi e^2}{k_B}\left(\frac{n_{e0}}{T_e} + \frac{n_{i0}}{T_i}\right). \tag{9}$$

Clearly, for $A = B = 0$, (8) yields the dispersion relation for the DAW in an ideal dusty plasma (Rao *et al.* 1990):

$$\frac{\omega^2}{k^2} = \frac{C_{DA}^2}{1 + k^2\lambda_D^2} + V_{td}^2, \tag{10}$$

where $C_{DA} \equiv \omega_{pd}\,\lambda_D$ is the usual DAW phase speed.

Substituting for the parameters A and B from (7), the dispersion relation (8) in the long-wavelength limit ($k\,\lambda_D \ll 1$) becomes

$$\frac{\omega^2}{k^2\,C_D^2} = 1 + \epsilon_{vr} + \epsilon_{cf}, \tag{11}$$

where $\alpha = T_c/T_d$, $\beta = V_{td}^2/C_D^2$, $\eta = n_{d0}/n_c$ and $C_D^2 = C_{DA}^2 + V_{td}^2$, and the quantities ϵ_{vr} and ϵ_{cf}, which are defined by

$$\epsilon_{vr} = \frac{\beta\eta\,(6-\eta)}{(3-\eta)^2}, \qquad \epsilon_{cf} = -\frac{9\,\alpha\beta\eta}{4}, \tag{12}$$

denote respectively the contributions due to the volume reduction coefficient and to the molecular cohesive forces, which are parameterized in terms of the quantities η and α. Clearly, in the high-temperature limit ($\alpha \to 0$) for a dilute gas ($\eta \to 0$), these contributions tend to zero, and we readily recover the results of the ideal-gas model for the dust component. The net contribution $\epsilon = \epsilon_{vr} + \epsilon_{cf}$ due to the non-ideal nature of the gas depends, as discussed below, on specific parameter values. However, in order that the normal-mode structure be maintained, it is necessary that $|\epsilon| < 1$ when ϵ is negative.

Figures 1 and 2 show the plots of ϵ_{vr} and ϵ_{cf} for typical parameter values, while in Fig. 3 we plot the total contribution to the DAW phase speed as a function of η. It follows from Fig. 1 that the contribution due to the volume reduction coefficient is positive, and hence it increases the phase speed of the DAW. This can be explained physically by the fact that the volume reduction results in increased gas pressure (cf. (6)), which enhances the restoring force for driving the wave motion. On the other hand, the van der Waals molecular cohesive forces reduce the gas pressure, and therefore the contribution due to the term ϵ_{cf} is negative (cf. Fig. 2). The net result of the two effects depends on the parameters α and η. From Fig. 3, it is clear that for $\alpha \ll 1$, there is an increase in the DAW phase speed for sub- as well as supercritical values of η. For larger values of α, the contribution due to the cohesive forces dominates resulting in a net decrease in the DAW phase speed.

4. Nonlinear waves

Nonlinear DAWs are governed by the full set of equations (1)–(4) and (6). For small but finite amplitudes, these equations can be analysed perturbatively to yield nonlinear evolution equations of the Boussinesq or the KDV type as in the ideal-gas

https://doi.org/10.1017/S0022377898006473 Published online by Cambridge University Press

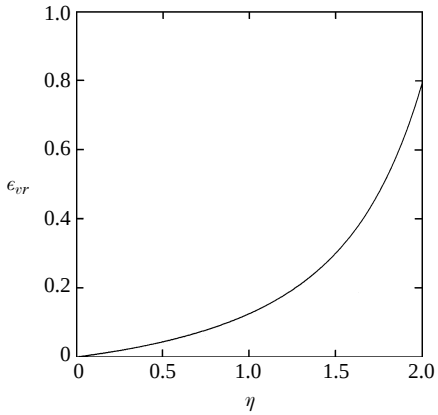


Figure 1. Plot, as a function of η, of the contribution ϵ_{vr} to the normalized dust-acoustic phase speed arising from the volume reduction coefficient. Note that ϵ_{vr} is positive, since the volume reduction coefficient leads to an increase in the gas pressure. $\beta = 0.1$.

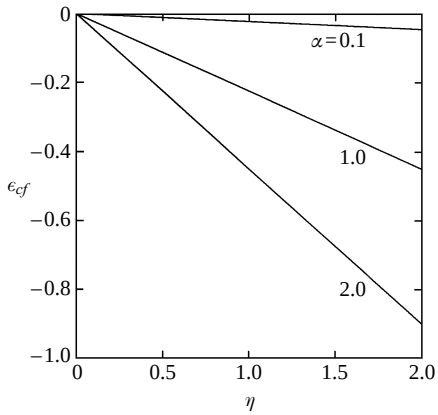


Figure 2. Plot, as a function of η, of the contribution ϵ_{cf} to the normalized dust-acoustic phase speed arising from the cohesive forces. Note that ϵ_{cf} is negative, since the cohesive forces reduce the gas pressure. $\beta = 0.1$.

case (Rao *et al.* 1990). For stationary propagation, these equations admit soliton-type localized solutions. For large amplitudes, such an analysis is not applicable. However, for stationary propagation with respect to a frame $\xi = x - Mt$, where M characterizes the propagation speed, the stationary equations can be integrated and exactly reduced to a Hamiltonian form, which represents the 'energy integral' for the motion of a quasiparticle in a potential called the 'Sagdeev potential' (Chen 1984). From an analysis of the latter, it is possible to obtain the existence relations and to establish the nature of the solutions admissible for the stationary governing equations. We consider the two cases separately below.

4.1. Large-amplitude case

To obtain the exact Sagdeev potential for stationary propagation, we transform (2)–(4) into the stationary frame, integrate once with respect to ξ, and combine using (1) and (6). The procedure is quite straightforward, although the algebra is fairly cumbersome. In particular, it should be pointed out that it is possible to

https://doi.org/10.1017/S0022377898006473 Published online by Cambridge University Press

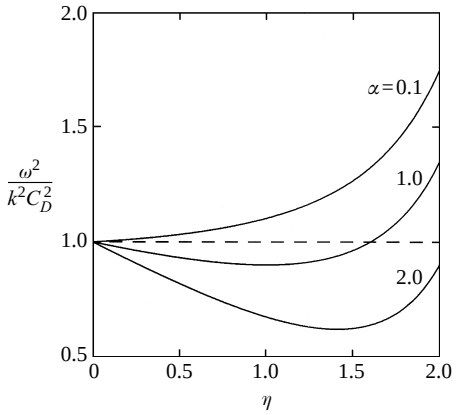


Figure 3. Normalized dust-acoustic phase speed ω/kC_D as a function of η. The dashed line corresponds to the case of an ideal gas. $\beta = 0.1$.

obtain the energy integral when the variables v_d, p_d and ϕ are eliminated in favour of the number density variable n_d. Omitting the details, we write the final equation in the form

$$\frac{1}{2}\left(\frac{dn_d}{d\xi}\right)^2 + V(n_d) = 0, \tag{13}$$

where the Sagdeev potential $V(n_d)$ is defined by

$$V(n_d) = -\frac{1}{F_1^2}\left[\frac{9(n_d-1)}{(3-\eta n_d)(3-\eta)} + \frac{9\alpha\eta}{8}(1-n_d^2) + \frac{M^2}{\beta n_d}(1-n_d) + \sigma_i\delta(e^{-\Phi_i}-1) + \sigma_e(\delta+Z_d)(e^{\Phi_e}-1)\right], \tag{14}$$

where

$$F_1 = \frac{9\,\alpha\beta\eta}{4} - \frac{9\beta}{n_d}\frac{1}{(3-\eta n_d)^2} + \frac{M^2}{n_d^3}, \tag{15}$$

$$\Phi_e = \frac{F_2}{Z_d\sigma_e\beta}, \qquad \Phi_i = \frac{F_2}{Z_d\sigma_i\beta}, \tag{16}$$

$$F_2 = \frac{M^2}{2n_d^2}(n_d^2-1) + \beta\ln\left[\frac{(3-\eta n_d)}{n_d\,(3-\eta)}\right] + \frac{3\eta\beta(1-n_d)}{(3-\eta n_d)(3-\eta)} + \frac{9\alpha\beta\eta}{4}(n_d-1). \tag{17}$$

In (13)–(17), we have defined $\delta = n_{i0}/n_{d0}$, $\sigma_i = k_BT_i/k_dT_d$ and $\sigma_e = k_BT_e/k_dT_d$, and have normalized M, n_d and ξ with respect to C_D, n_{d0} and $C_D^2/\omega_{pd}V_{td}$ respectively. For $\alpha = \eta = 0$, (14) yields the Sagdeev potential for the ideal-gas case (Singh and Rao 1997).

The potential $V(n_d)$ given by (13) can be analysed to obtain the parameter regimes for the existence of large-amplitude solitons (Chen 1984). Localized solutions for the dust number density are possible provided that $V(n_d) < 0$ in some range of n_d around $n_d = 1$ such that $V(n_d = 1) = V(n_d = n_m) = 0$ with a maximum at $n_d = 1$. This is supplemented by the requirement that $\partial V/\partial n_d > 0\,(< 0)$ at $n_d = n_m$ for $n_m > 1\,(< 1)$. Since, in the neighbourhood of $n_d = 1$, $V(n_d) \sim -\frac{1}{2}\lambda_1\,(n_d-1)^2$, where λ_1 is defined in Sec. 4.2 it follows that $\lambda_1 > 0$ is required in order that $V(n_d)$

https://doi.org/10.1017/S0022377898006473 Published online by Cambridge University Press

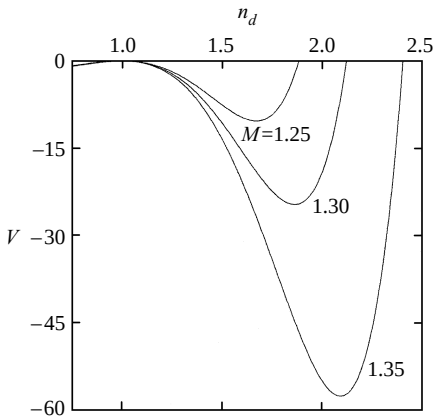


Figure 4. Sagdeev potential for the subcritical ($\alpha, \eta < 1$) case when large-amplitude supersonic ($M > 1$) solitons are admissible. $\alpha = \eta = 0.1$, $\delta = 10^5$, $\beta = 0.01$, $\sigma_e = 100$, $\sigma_i = 10$ and $Z_d = -1000$.

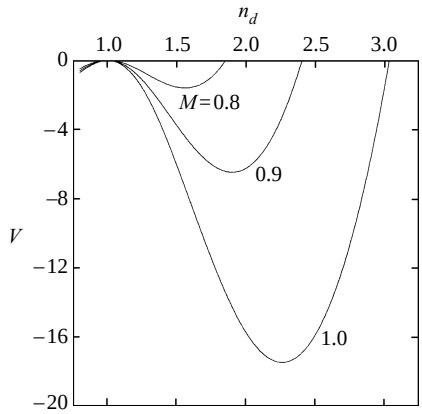


Figure 5. Sagdeev potential for the supercritical ($\alpha, \eta > 1$) case for the existence of large-amplitude subsonic ($M < 1$) solitons. $\alpha = \eta = 5$; the other parameters are as in Fig. 4.

have a maximum at $n_d = 1$. Clearly, the DAW solitons are associated with density compressions (rarefactions) according as $n_m > 1\ (< 1)$.

Figures 4–6 show typical plots of the Sagdeev potential for different values of α and η. Depending on the parameter values, large-amplitude solitons exist in both the subsonic ($M < 1$) and the supersonic ($M > 1$) regimes. Soliton propagation with supersonic Mach numbers is possible for both the subcritical (η, $\alpha < 1$) and the supercritical (η, $\alpha > 1$) parameter regimes. On the other hand, propagation in the near-sonic regime with $M \lesssim 1$ is admissible only for the supercritical case. These are associated with compressional density perturbations ($n_d > 1$). Analysis of the Sagdeev potential shows that for $\eta \ll 1$, spiky solitons associated with density rarefactions are possible in the near-static ($M \ll 1$) regime. Explicit solutions for the solitons can be derived by the usual method of quadratures on the energy integral (13). However, for small but finite amplitudes, analytical solutions can be obtained. This is discussed in the next subsection.

https://doi.org/10.1017/S0022377898006473 Published online by Cambridge University Press

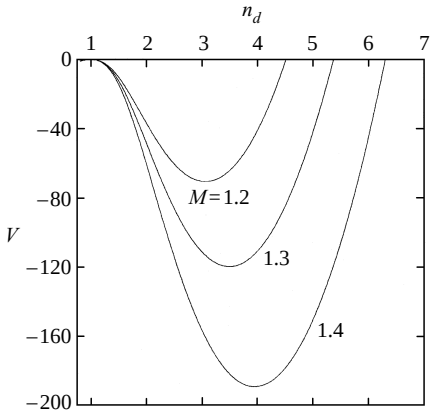


Figure 6. Sagdeev potential for the supercritical ($\alpha, \eta > 1$) case for the existence of large-amplitude supersonic ($M > 1$) solitons. $\alpha = \eta = 5$; the other parameters are as in Fig. 4.

4.2. Small- but finite-amplitude case

As mentioned earlier, for small but finite amplitudes, the governing equations (1)–(4) and (6) can be reduced to a tractable nonlinear evolution equation of the KDV type for unidirectional propagation, and, more generally, to the Boussinesq equation for bidirectional propagation. The stationary form of the latter equation can also be obtained directly from the energy integral (13) by expanding the various quantities in terms of the dust density perturbation $N = n_d - 1$, where N is normalized with respect to n_{d0}. Equation (13) then reduces to

$$\left(\frac{dN}{d\xi}\right)^2 = \lambda_1 N^2 + \frac{2\lambda_2}{3} N^3 + \frac{\lambda_3}{2} N^4, \tag{18}$$

where the coefficients λ_1, λ_2 and λ_3 are given in the Appendix. Equation (18) admits a pair of localized solutions (Davis 1962)

$$N_\pm(\xi) = \frac{\beta_\pm \beta_\mp \operatorname{sech}^2[\mu(\xi - \xi_0)]}{\beta_\pm - \beta_\mp \tanh^2[\mu(\xi - \xi_0)]}, \tag{19}$$

where ξ_0 is the constant of integration, $\mu = \frac{1}{2}\lambda_1^{-1/2}$, and the coefficients β_+ and β_- are defined by

$$\begin{pmatrix} \beta_+ \\ \beta_- \end{pmatrix} = \frac{1}{3\lambda_3}[-2\lambda_2 \pm (4\lambda_2^2 - 18\lambda_1\lambda_3)^{1/2}]. \tag{20}$$

For admissible solutions, one requires, $\lambda_1 > 0$, $\lambda_2 \neq 0$, $\lambda_3 > 0$, and $\beta_+ \neq \pm\beta_- \neq 0$. It may be noted that, as pointed out in Sec. 4.1, the requirement $\lambda_1 > 0$ is also needed for large-amplitude waves.

The choice of the solutions $N_\pm(\xi)$ is governed by the values of λ_2. In order that the solutions be finite everywhere, it is necessary to choose $N_+(\xi)$ for $\lambda_2 < 0$ and $N_-(\xi)$ for $\lambda_2 > 0$. From the definitions (20), it follows that $\beta_\pm > 0$ with $\beta_+ > \beta_-$ for $\lambda_2 < 0$, and $\beta_\pm < 0$ with $|\beta_-| > |\beta_+|$ for $\lambda_2 > 0$. The solutions $N_\pm(\xi)$ can be analysed for the structure of the soliton profiles. Each is localized, having an extremum at $\xi = \xi_0$. Since, from (19), $N_\pm(\xi = \xi_0) = \beta_\mp$, it follows that N_+ (N_-) has a single-hump (single-dip) structure that is positive (negative) everywhere for

https://doi.org/10.1017/S0022377898006473 Published online by Cambridge University Press

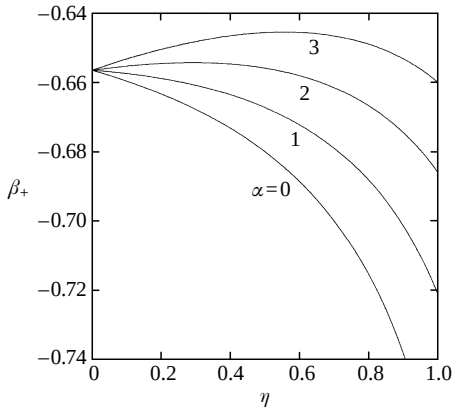


Figure 7. Plot of β_+ as a function of η for different values of α for the supersonic case when $\lambda_2 > 0$. The admissible localized solution for the latter is $N_-(\xi)$, which has the amplitude β_+. $M = 1.4$, $\delta = 10^5$, $\beta = 0.01$, $\sigma_e = 100$, $\sigma_i = 10$ and $Z_d = -1000$.

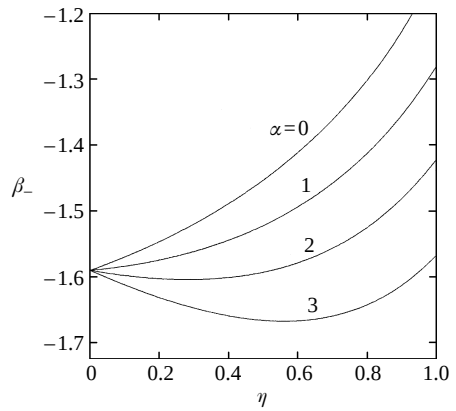


Figure 8. Plot of β_- as a function of η for different values of α for the supersonic case when $\lambda_2 > 0$. Parameters are as in Fig. 7.

$\lambda_2 < 0$ (> 0). Figures 7 and 8 show the variations of β_+ and β_- as functions of η for the case when $\lambda_2 > 0$.

We close this section by briefly discussing a limiting case of (18) that leads to the usual sech^2 type of solutions. To obtain these, we neglect the last term on the right-hand side of (18) and obtain

$$\left(\frac{dN}{d\xi}\right)^2 = \lambda_1 N^2 + \frac{2\lambda_2}{3} N^3, \tag{21}$$

which has the solution

$$N(\xi) = N_0 \,\mathrm{sech}^2\left[\mu(\xi - \xi_0)\right], \tag{22}$$

where $N_0 = -3\lambda_1/2\lambda_2$ and $\mu = \frac{1}{2}\lambda_1^{1/2}$. As before we require $\lambda_1 > 0$, while the sign of N_0 depends on the sign of λ_2. In order to recover the solution (22) from (19) and thereby determine the condition for its validity, we take in (20) the limit $\lambda_3 \to 0$ such that $|9\lambda_1\lambda_3| \ll 2\lambda_2^2$. It is then easy to verify that the solution N_+ (N_-) yields exactly the solution (22) for $\lambda_2 < 0$ (> 0). Figure 9 shows a plot

https://doi.org/10.1017/S0022377898006473 Published online by Cambridge University Press

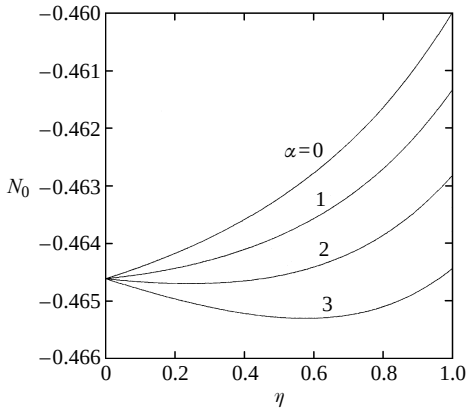


Figure 9. Plot of the amplitude N_0 for the solution (22) as a function of η. Parameters are as in Fig. 7.

of N_0 for parameter values corresponding to Figs 7 and 8. Since $\lambda_2 > 0$ in this case, the amplitude of the solution $N_-(\xi)$ is equal to β_+. Thus, on comparing the corresponding curves in Figs 7 and 9, we note that, for typical parameter values, the solution (22) underestimates the soliton amplitude when compared with that of the solution (19). This is consistent with the fact that the latter includes a higher-order nonlinear term.

5. Summary

We have investigated the propagation of linear and nonlinear dust-acoustic waves (DAWs) in a non-ideal classical dusty plasma wherein the electrons and the ions are assumed to behave like ideal fluids while the dust component is described by the van der Waals equation of state. The effect of the latter manifests itself in two contributions. First, the volume reduction coefficient, which can be appreciable for large grain sizes, leads to an increase in the phase speed of the dust-acoustic waves. This is in agreement with the fact that volume reduction increases the gas pressure, which enhances the restoring force driving the wave. Secondly, the molecular cohesive forces reduce the phase speed, since their contribution is to decrease the gas pressure. For nonlinear waves, we have considered the full set of governing equations together with the Poisson equation, and have shown that they can be reduced to quadrature. The Sagdeev potential thus obtained shows that large-amplitude DAW solitons are possible in both the sub- and supersonic regimes. For small but finite amplitudes, we have obtained explicit analytical solutions. A limiting case of the latter has also been discussed.

Acknowledgements

The author is grateful to a referee for making an important suggestion about possible physical mechanisms causing the cohesive forces between dust particles, and for pointing out the relevant references. This work was partially supported by the International Center for Theoretical Physics, Trieste under its Associate Membership Program.

https://doi.org/10.1017/S0022377898006473 Published online by Cambridge University Press

Appendix. Expansion coefficients λ_1, λ_2 and λ_3 in (18)

The expansion coefficients λ_1, λ_2 and λ_3 in (18) are given by

$$\left.\begin{aligned}\lambda_1 &= 2\,e_2/d_0^2,\\ \lambda_2 &= 3\,(e_2\,g_1 + e_3)/d_0^2,\\ \lambda_3 &= 4\,(e_2\,g_2 + e_3 g_1 + e_4)/d_0^2,\end{aligned}\right\} \tag{A 1}$$

where

$$\left.\begin{aligned}g_1 &= -2d_1/d_0,\\ g_2 &= (-2d_0d_2 + 3d_1^2)/d_0^2,\\ g_3 &= (-2d_0^2d_3 + 6d_0d_1d_2 - 4d_1^3)/d_0^3,\\ g_4 &= (-2d_0^3d_4 + 6d_0^2d_1d_3 + 3d_0^2d_2^2 - 12d_0d_1^2d_2 + 5d_1^4)/d_0^4,\end{aligned}\right\} \tag{A 2}$$

$$\left.\begin{aligned}e_1 &= a_1^2 - \frac{9\,\alpha\eta}{4} - \frac{M^2}{\beta} + b_1 + c_1 \equiv 0,\\ e_2 &= \mu a_1^2 - \frac{9\,\alpha\eta}{8} + \frac{M^2}{\beta} + b_2 + c_2,\\ e_3 &= \mu^2 a_1^2 - \frac{M^2}{\beta} + b_3 + c_3,\\ e_4 &= \mu^3 a_1^2 + \frac{M^2}{\beta} + b_4 + c_4,\end{aligned}\right\} \tag{A 3}$$

$$\left.\begin{aligned}d_0 &= \tfrac{9}{4}\alpha\beta\eta - \beta a_1^2 + M^2,\\ d_1 &= -\beta a_1^2(2\mu - 1) - 3M^2,\\ d_2 &= -\beta a_1^2(3\mu^2 - 2\mu + 1) + 6M^2,\\ d_3 &= -\beta a_1^2(4\mu^3 - 3\mu^2 + 2\mu - 1) - 10M^2,\\ d_4 &= -\beta a_1^2(5\mu^4 - 4\mu^3 + 3\mu^2 - 2\mu + 1) + 15M^2,\end{aligned}\right\} \tag{A 4}$$

$$\left.\begin{aligned}c_1 &= -\frac{\delta}{Z_d\beta}\,f_1,\\ c_2 &= \frac{\delta}{Z_d\beta}\left(\frac{f_1^2}{2Z_d\sigma_i\beta} - f_2\right),\\ c_3 &= \frac{\delta}{Z_d\beta}\left[-\frac{f_1^3}{6(Z_d\sigma_i\beta)^2} + \frac{f_1f_2}{Z_d\sigma_i\beta} - f_3\right],\\ c_4 &= \frac{\delta}{Z_d\beta}\left[\frac{f_1^4}{24(Z_d\sigma_i\beta)^3} - \frac{f_1^2f_2}{2(Z_d\sigma_i\beta)^2} + \frac{2f_1f_3 + f_2^2}{2Z_d\sigma_i\beta} - f_4\right],\end{aligned}\right\} \tag{A 5}$$

$$\left.\begin{aligned}b_1 &= \frac{\delta + Z_d}{Z_d\beta}\,f_1,\\ b_2 &= \frac{\delta + Z_d}{Z_d\beta}\left(\frac{f_1^2}{2Z_d\sigma_e\beta} + f_2\right),\\ b_3 &= \frac{\delta + Z_d}{Z_d\beta}\left[\frac{f_1^3}{6(Z_d\sigma_e\beta)^2} + \frac{f_1f_2}{Z_d\sigma_e\beta} + f_3\right],\\ b_4 &= \frac{\delta + Z_d}{Z_d\beta}\left[\frac{f_1^4}{24(Z_d\sigma_e\beta)^3} + \frac{f_1^2f_2}{2(Z_d\sigma_e\beta)^2} + \frac{2f_1f_3 + f_2^2}{2Z_d\sigma_e\beta} + f_4\right],\end{aligned}\right\} \tag{A 6}$$

https://doi.org/10.1017/S0022377898006473 Published online by Cambridge University Press

$$\left.\begin{aligned} f_1 &= M^2 + \beta a_1(1 - \tfrac{1}{3}\eta\, a_1) + \tfrac{9}{4}\alpha\beta\eta, \\ f_2 &= -\tfrac{3}{2}M^2 - \beta a_1(1 + \tfrac{1}{2}a_1) - \tfrac{1}{3}\eta\beta\,\mu a_1^2, \\ f_3 &= 2M^2 + \beta a_1(1 + a_1 + \tfrac{1}{3}a_1^2) - \tfrac{1}{3}\eta\beta\mu^2 a_1^2, \\ f_4 &= -\tfrac{5}{2}M^2 - \beta a_1\,(1 + \tfrac{3}{2}a_1 + a_1^2 + \tfrac{1}{4}a_1^3) - \tfrac{1}{3}\eta\beta\mu^3 a_1^2, \end{aligned}\right\} \tag{A 7}$$

$$a_1 = -(1 + \mu), \qquad \mu = \tfrac{1}{3}\eta(1 - \tfrac{1}{3}\eta)^{-1}. \tag{A 8}$$

References

Barkan, A., Merlino, R. L. and D'Angelo, N. 1995 *Phys. Plasmas* **2**, 3563.

Benkadda, S., Tsytovich, V. N. and Verga, A. 1995 *Comments Plasma Phys. Cont. Fusion* **16**, 321.

Bharuthram, R. and Shukla, P. K. 1992*a* *Planet. Space Sci.* **40**, 465.

Bharuthram, R. and Shukla, P. K. 1992*b* *Planet. Space Sci.* **40**, 647.

Bouchoule, A., Plain, A., Boufendi, L., Blondeau, J. Ph. and Laure, C. 1991 *J. Appl. Phys.* **70**, 1991.

Carlile, R. N., Gehe, S., O'Hanlon, J. F. and Stewart, J. C. 1991 *Appl. Phys. Lett.* **59**, 1167.

Chen, F. F. 1984 *Introduction to Plasma Physics and Controlled Fusion*, Vol. 1. Plenum, New York.

Chu, J. H. and Lin, I. 1994 *Phys. Rev. Lett.* **72**, 4009.

Chu, J. H., Du, J. B. and Lin, I. 1994 *J. Phys.* **D27**, 296.

D'Angelo, N. 1993 *Planet. Space Sci.* **41**, 469.

D'Angelo N. 1995 *J. Phys.* **D28**, 1009.

Davis, H. T. 1962 *Introduction to Nonlinear Differential and Integral Equations*. Dover, New York.

De Angelis, U., Formisano, V. and Giordano, M. 1988 *J. Plasma Phys.* **40**, 399.

Fortov, V. E. and Iakubov, I. T. 1990 *Physics of Nonideal Plasmas*. Hemisphere, New York.

Goertz, C. K. 1989 *Rev. Geophys.* **27**, 271.

Havnes, O., Melandsø , F., La Hoz, C., Aslaksen, T. K. and Hartquist, T. 1992 *Physica Scripta* **45**, 535.

Hayashi,Y. and Tachibana, K. 1994 *Jpn J. Appl. Phys.* **33**, L804.

Hirschfelder, J. O., Curtiss, C. F. and Bird, R. B. 1954 *Molecular Theory of Gases and Liquids*, p. 250. Wiley, New York.

Ikezi, H. 1986 *Phys. Fluids* **29**, 1764.

Jana, M. R., Sen, A. and Kaw, P. K. 1993 *Phys. Rev.* **E48**, 3930.

Joos, G. 1986 *Theoretical Physics*, p. 497. Dover, New York.

Kahn, B. 1965 *Studies in Statistical Mechanics*, Vol. III (ed. J. De Boer, and G. E. Uhlenbeck), p. 289. North-Holland, Amsterdam.

Kennard, E. H. 1938 *Kinetic Theory of Gases*, p. 206. McGraw-Hill, New York.

Melandsø , F. and Goree, J. 1995 *Phys. Rev.* **E52**, 5312.

Melandsø , F., Aslaksen, T. K. and Havnes, O. 1993 *J. Geophys. Res.* **98**, 13 315.

Mendis, D. A. and Rosenberg, M. 1994 *Annu. Rev. Astron. Astrophys.* **32**, 419.

Motschmann, U., Sauer, K. and Roatsch, T. 1992 *Geophys. Res. Lett.* **19**, 225.

Nambu, M., Vladimirov, S. V. and Shukla, P. K. 1995 *Phys. Lett.* **203A**, 40.

Pieper, J. B. and Goree, J. 1996 *Phys. Rev. Lett.* **77**, 3137.

Prabhakara, H. R. and Tanna, V. L. 1996 *Phys. Plasmas* **3**, 3176.

Prabhuram, G. and Goree, J. 1996 *Phys. Plasmas* **3**, 1212.

Rao, N. N. 1993*a* *J. Plasma Phys.* **49**, 375.

Rao, N. N. 1993*b* *Planet. Space Sci.* **41**, 21.

Rao, N. N. and Shukla, P. K. 1994 *Planet. Space Sci.* **42**, 221.

Rao, N. N., Shukla, P. K. and Yu, M. Y. 1990 *Planet. Space Sci.* **38**, 543.

https://doi.org/10.1017/S0022377898006473 Published online by Cambridge University Press

Rawat, S. P. S. and Rao, N. N. 1993 *Planet. Space Sci.* **41**, 137.
Rosenberg, M. 1993 *Planet. Space Sci.* **41**, 229.
Sheehan, D. P., Carillo, M. and Heidbrink, W. 1990 *Rev. Sci. Instrum.* **61**, 3871.
Shukla, P. K. 1992 *Physica Scripta* **45**, 504.
Shukla, P. K. and Rao, N. N. 1996 *Phys. Plasmas* **3**, 1770.
Shukla, P. K. and Silin, V. P. 1992 *Physica Scripta* **45**, 508.
Singh, S. V. and Rao, N. N. 1997 *Phys. Lett.* **235A**, 164.
Thomas, H., Morfill, G. E., Demmel, V., Goree, J., Feuerbach, B. and Möhlmann, D. 1994 *Phys. Rev. Lett.* **73**, 652
Varma, R. K., Shukla, P. K. and Krishan, V. 1993 *Phys. Rev.* **E47**, 3612.
Verheest, F. 1996 *Space Sci. Rev.* **77**, 267.

https://doi.org/10.1017/S0022377898006473 Published online by Cambridge University Press